⌘ *Author's Choice*

THE JOURNAL OF BIOLOGICAL CHEMISTRY VOL. 284, NO. 26, pp. 17457–17464, June 26, 2009

Mechanism of Inhibition by C-terminal α-Helices of the ε Subunit of *Escherichia coli* F_oF_1-ATP Synthase*

Received for publication, January 28, 2009, and in revised form, April 3, 2009 Published, JBC Papers in Press, May 1, 2009, DOI 10.1074/jbc.M109.003798

Ryota Iino[1], **Rie Hasegawa, Kazuhito V. Tabata, and Hiroyuki Noji**[2]

From the Institute of Scientific and Industrial Research, Osaka University, 567-0047 Osaka, Japan

The ε subunit of bacterial F_oF_1-ATP synthase (F_oF_1), a rotary motor protein, is known to inhibit the ATP hydrolysis reaction of this enzyme. The inhibitory effect is modulated by the conformation of the C-terminal α-helices of ε, and the "extended" but not "hairpin-folded" state is responsible for inhibition. Although the inhibition of ATP hydrolysis by the C-terminal domain of ε has been extensively studied, the effect on ATP synthesis is not fully understood. In this study, we generated an *Escherichia coli* F_oF_1 (EF_oF_1) mutant in which the ε subunit lacked the C-terminal domain ($F_oF_1^{\epsilon\Delta C}$), and ATP synthesis driven by acid-base transition (ΔpH) and the K^+-valinomycin diffusion potential (ΔΨ) was compared in detail with that of the wild-type enzyme ($F_oF_1^{\epsilon WT}$). The turnover numbers (k_{cat}) of $F_oF_1^{\epsilon WT}$ were severalfold lower than those of $F_oF_1^{\epsilon\Delta C}$. $F_oF_1^{\epsilon WT}$ showed higher Michaelis constants (K_m). The dependence of the activities of $F_oF_1^{\epsilon WT}$ and $F_oF_1^{\epsilon\Delta C}$ on various combinations of ΔpH and ΔΨ was similar, suggesting that the rate-limiting step in ATP synthesis was unaltered by the C-terminal domain of ε. Solubilized $F_oF_1^{\epsilon WT}$ also showed lower k_{cat} and higher K_m values for ATP hydrolysis than the corresponding values of $F_oF_1^{\epsilon\Delta C}$. These results suggest that the C-terminal domain of the ε subunit of EF_oF_1 slows multiple elementary steps in both the ATP synthesis/hydrolysis reactions by restricting the rotation of the γ subunit.

F_oF_1-ATP synthase (F_oF_1)[3] is an enzyme that is responsible for ATP synthesis during oxidative phosphorylation and photosynthesis (1–3). F_oF_1 is a complex of two rotary motors F_1 and F_o, and the ATP synthesis/hydrolysis reaction that is reversibly catalyzed by F_1 is coupled with proton transport across membrane-embedded F_o (4–6). The subunit composition of bacterial F_1 and F_o is $\alpha_3\beta_3\gamma\delta\epsilon$ and ab_2c_{10-15}, respectively, and the $\gamma\epsilon c_{10-15}$ complex rotates against the $\alpha_3\beta_3\delta ab_2$ complex in F_oF_1.

Among these subunits, ε is known to be an endogenous inhibitor of the ATP hydrolysis reaction catalyzed by F_1 and F_oF_1 (7–10). The inhibition of ATP hydrolysis by the ε subunit of *Escherichia coli* F_1 (EF_1) and F_oF_1 (EF_oF_1) has been extensively studied. Addition of ε to ε-depleted EF_1 showed noncompetitive inhibition of ATP hydrolysis (7). The affinity of MgATP and MgADP to the high affinity site of the three catalytic β subunits of EF_1 was decreased by ε (11). It has been reported that the ε subunit of EF_1 had no effect on the equilibrium between ATP and ADP·P_i but inhibited product release under unisite catalysis conditions (12). Inhibition of EF_oF_1-mediated ATP hydrolysis by ε was also demonstrated in experiments involving partial digestion by a protease (13). The inhibitory effect of the ε subunit of thermophilic *Bacillus* PS3 F_1 (TF_1) and F_oF_1 (TF_oF_1) has also been studied extensively. Slow binding and hydrolysis of TNP-ATP, a fluorescent ATP analog, under unisite catalysis conditions have been reported (14). However, in contrast to EF_1, inhibition by the ε subunit of TF_1 was relieved slowly and apparently disappeared at high ATP concentrations ([ATP]). This is not due to the dissociation of ε from the F_1 complex, because disappearance of inhibition at high [ATP] was also reported in TF_oF_1 in which ε is indispensable for stable complex formation (15). However, in contrast to ATP hydrolysis, there has been no detailed analysis of the effect of ε on ATP synthesis.

The ε subunit has a molecular mass of 14 kDa and a two-domain structure consisting of an N-terminal 10-stranded β-sandwich and two C-terminal α-helices. Of these two domains, the C-terminal domain is responsible for inhibiting ATP hydrolysis, and the ε subunit in which this domain is absent does not have any inhibitory effect (15, 16). Structural studies on isolated ε and its complex with the truncated γ subunit have shown that the C-terminal domain of ε adopts two different conformations, the "hairpin-folded" and "extended" states (Fig. 1) (17–20). These conformations are also found in the crystal structure of the bovine mitochondrial homolog of F_1 and in the low resolution crystal structure of EF_1 (21, 22). Chemical modification of the ε subunit of EF_oF_1 indicated that the C-terminal domain is intrinsically flexible (23). Cross-linking and fluorescence resonance energy transfer experiments supported the existence of multiple conformations of the ε subunit of EF_oF_1 and TF_oF_1 (24–30).[4] These studies have shown that the extended state inhibits ATP hydrolysis, whereas the hairpin-folded state does not.

In contrast to ATP hydrolysis, the correlation between the

* This work was supported in part by Grants-in-aid for Scientific Research 18770134 and 18074005 (to R. I. and H. N., respectively) from the Ministry of Education, Culture, Sports, Science and Technology, Japan.

⌘ *Author's Choice*—Final version full access.

[1] To whom correspondence may be addressed. Tel.: 81-6-6879-8481; Fax: 81-6-6875-5724; E-mail: iino@sanken.osaka-u.ac.jp.

[2] To whom correspondence may be addressed. Tel.: 81-6-6879-8481; Fax: 81-6-6875-5724; E-mail: hnoji@sanken.osaka-u.ac.jp.

[3] The abbreviations used are: F_oF_1, F_oF_1-ATP synthase; F_1, F_1-ATPase; EF_oF_1, F_oF_1 from *E. coli*; EF_1, F_1 from *E. coli*; TF_oF_1, F_oF_1 from thermophilic *Bacillus* PS3; TF_1, F_1 from thermophilic *Bacillus* PS3; $F_oF_1^{\epsilon\Delta C}$, F_oF_1 lacking the two α-helices at the C terminus of the ε subunit; $F_oF_1^{\epsilon WT}$, wild-type F_oF_1; $C_{12}E_8$, octaethylene glycol mono-*n*-dodecyl ether; PAB, 4-aminobenzamidine dihydrochloride; TNP-ATP, 2′(3′)-*O*-(2,4,6-trinitrophenyl)adenosine 5′-triphosphate.

[4] Another kind of "extended" state was proposed in TF_oF_1 (27); however, for simplicity, we did not distinguish between the two extended forms in this manuscript.

conformation of ϵ and its effect on ATP synthesis has not been fully understood. In both EF_oF_1 and TF_oF_1, when ϵ was fixed in an extended state that inhibits ATP hydrolysis, no change was observed in the ATP synthesis activity driven by the proton motive force ($\Delta\mu$) generated by the respiratory chain in the inverted membrane (26, 27). Based on these results, it has been proposed that ϵ functions as a ratchet that inhibits only ATP hydrolysis. However, Masaike *et al.* (31) reported that truncation of the C-terminal domain of ϵ increased the ATP synthesis activity of TF_oF_1, suggesting that the C-terminal domain of ϵ suppresses the ATP synthesis activity.

In this study, we generated an EF_oF_1 mutant with a truncated ϵ subunit that did not contain the C-terminal α-helices ($F_oF_1^{\epsilon\Delta C}$). This mutant was purified and reconstituted into a liposome, and the ATP synthesis rate was measured by the acid-base transition (ΔpH) and K^+-valinomycin diffusion potential ($\Delta\Psi$) methods. The rate of ATP hydrolysis by solubilized EF_oF_1 was also measured. The activities of $F_oF_1^{\epsilon\Delta C}$ under various conditions were investigated and compared in detail with those of the wild-type enzyme ($F_oF_1^{\epsilon WT}$). The results indicated that the ATP synthesis and hydrolysis activities of $F_oF_1^{\epsilon\Delta C}$ were much higher than those of $F_oF_1^{\epsilon WT}$. The inhibitory mechanism of the C-terminal α-helices of the ϵ subunit of EF_oF_1 was discussed.

EXPERIMENTAL PROCEDURES

Construction and Expression of the EF_oF_1 Mutant—A wild-type EF_oF_1 expression vector (pRA100) (32) was provided by Prof. R. A. Capaldi, University of Oregon. Based on this vector, a 1.3 S subunit of *Propionibacterium shermanii* transcarboxylase (33) was fused to the N terminus of the β subunits, and three histidine residues were introduced at the C terminus of the c subunits. This mutant is referred to as the wild-type (denoted by $F_oF_1^{\epsilon WT}$) hereafter. F_oF_1 lacking the two α-helices in the C terminus of the ϵ subunit (denoted by $F_oF_1^{\epsilon\Delta C}$) was generated by introducing a stop codon at the position of Asp-91.

RA1 strain *E. coli* (*unc*$^-$/*cyo*$^-$) (34) was transformed with the F_oF_1 mutant plasmid. After preculture in 5 ml of LB (1% tryptone, 0.5% yeast extract, and 1% NaCl) containing 30 μg/ml chloramphenicol for 8–9 h at 37 °C, the cells were inoculated in 1.2 liters of TB (1.2% tryptone, 2.4% yeast extract, 0.4% glycerol, 1.25% K_2HPO_4, and 0.23% KH_2PO_4) containing 30 μg/ml chloramphenicol and then cultured for 16 h at 37 °C.

Preparation of Inverted Membrane Vesicles—The cells were harvested and washed with buffer containing 100 mM HEPES-KOH (pH 7.5) and 50 mM KCl. The pellet was then resuspended in buffer A (100 mM HEPES-KOH (pH 7.5), 1 mM EDTA, 500 mM sucrose, 1 mM dithiothreitol, and 2× protease inhibitor mixture (Complete, Roche Applied Science)). Egg white lysozyme (8–12 mg, Seikagaku Corp.) was added, and the mixture was incubated at room temperature for 20 min. Subsequently, 1–2 mg of DNase I (Roche Applied Science) and 5 mM $MgCl_2$ were added, and incubation was carried out at 4 °C for 20 min. The spheroplasts were then spun down, resuspended in buffer B (50 mM HEPES-KOH (pH 7.5), 0.5 mM EDTA, 250 mM sucrose, 0.5 mM dithiothreitol, 5 mM $MgCl_2$, and 5 mM 4-aminobenzamidine dihydrochloride (PAB)), and sonicated (model CL4, Misonix) on ice. They were then centrifuged at 9000 rpm for 10 min at 4 °C to remove the cell debris. The supernatant containing the inverted membrane was transferred to a new tube and centrifuged at 75,000 rpm for 20 min at 4 °C. The supernatant was discarded, and the pellet was resuspended in buffer B at 250 mg/ml. The inverted membrane was stored at −80 °C prior to further use.

Purification of EF_oF_1—The membrane suspension (250 mg/ml, wet weight of inverted membrane/volume of buffer) in 0.8% (w/v) *n*-octyl β-D-glucopyranoside (Sigma) was centrifuged at 75,000 rpm for 20 min at 4 °C. The supernatant was transferred to a new tube on ice. Buffer C (20 mM HEPES-KOH (pH 7.5), 500 mM NaCl, 5 mM $MgCl_2$, 200 μM ADP, 50 mM imidazole, 20% (v/v) glycerol, 1× protease inhibitor mixture, and 5 mM PAB) and 2% (w/v) octaethylene glycol mono-*n*-dodecyl ether ($C_{12}E_8$, Wako) were added to the pellet, and the mixture was incubated for 15 min on ice. It was then centrifuged, and the supernatant was collected. The collected supernatant was injected into a HisTrap HP column (GE Healthcare) pre-equilibrated with 5 ml of buffer D (20 mM HEPES-KOH (pH 7.5), 500 mM NaCl, 5 mM $MgCl_2$, 200 μM ADP, 50 mM imidazole, 20% glycerol (v/v), 1× protease inhibitor mixture, 5 mM PAB, 0.3% (w/v) $C_{12}E_8$, and 0.1% (w/v) *E. coli* total lipid (Avanti)). The column was washed twice with 5 ml of buffer D. His-tagged EF_oF_1 was eluted with 3 ml of buffer E (20 mM HEPES-KOH (pH 7.5), 500 mM NaCl, 5 mM $MgCl_2$, 200 μM ADP, 500 mM imidazole, 20% glycerol (v/v), 1× protease inhibitor mixture, 5 mM PAB, 0.3% (w/v) $C_{12}E_8$, and 0.1% (w/v) *E. coli* total lipid). Six drops of the eluate were collected in each 1.5-ml tube containing 1 mM dithiothreitol. The purified EF_oF_1 fractions were run on 15% SDS-PAGE to select the purest fractions that contained all the subunits and the least contaminants. The chosen fractions were pooled and passed through a NAP-5 column (GE Healthcare) that had been pre-equilibrated with buffer F (20 mM HEPES-NaOH (pH 7.5), 100 mM NaCl, 2 mM $MgCl_2$, 0.1× protease inhibitor mixture, 5 mM PAB, 0.3% (w/v) $C_{12}E_8$, and 0.1% (w/v) *E. coli* total lipid). EF_oF_1 was eluted with 1 ml of buffer F. The eluate was concentrated and further purified in an Amicon Ultra-4 100,000 centrifugal filter device (Millipore). The protein concentration of the sample was determined by the BCA assay (Pierce) using bovine serum albumin (Sigma) as the standard. Purified EF_oF_1 was immediately used for reconstitution into the liposome or to measure the ATP hydrolysis activity.

Liposome Preparation and Reconstitution of EF_oF_1 into the Liposome—L-α-Phosphatidylcholine from soybean (type II-S, Sigma) was suspended in buffer G (10 mM HEPES-NaOH, 5 mM $MgSO_4$, and 1 mM KCl (pH 7.5)) by vigorous vortexing. The liposome suspension was then repeatedly freeze-thawed three times. The final concentration of the lipid was 40 mg/ml. Solubilized EF_oF_1 was reconstituted into the liposomes using the freeze-thaw method. The EF_oF_1 solution (~1 mg/ml, 100 μl) was added to the liposome suspension (40 mg/ml, 1 ml), and the mixture was frozen in liquid nitrogen and stored at −80 °C prior to further use. Reconstitution efficiency of EF_oF_1 into liposome was assessed by SDS-PAGE of EF_oF_1/liposome suspension and the supernatant after centrifugation of EF_oF_1/liposome at 75,000 rpm for 20 min at 4 °C.

Measurement of the ATP Synthesis Activity—The ATP synthesis activity was measured as described previously with slight

modifications (35). To acidify the interior of the proteoliposomes, 10 μl of the proteoliposome suspension was mixed with 50 μl of acidification buffer (300 mM MES-NaOH or HEPES-NaOH) and incubated for 3 min at room temperature. Following incubation, the pH of the acidified liposome suspension was measured by a glass electrode, and this value was regarded as the pH inside the liposome (pH_{in}). The ATP synthesis reaction was initiated by injecting 60 μl of the acidified proteoliposomes into 1 ml of base buffer containing 100 mM Tricine-Na (pH 8.8) or HEPES-NaOH (pH 7.5), 2.5 mM $MgSO_4$, 0.1–50 mM phosphate, 2.2 mg of luciferin/luciferase mixture from ATP Bioluminescence Assay Kit CLS II (Roche Applied Science), 0.001–1 mM ADP, 36 nM valinomycin, and 1–300 mM KCl. The amount of ATP generated was measured as the increase in the luminescence intensity of the luciferin/luciferase reaction at 550 nm in an FP-6500 spectrofluorometer (Jasco, Japan). The ATP synthesis rate was calculated using the initial slope of the increase in the luminescence intensity. To calibrate the system for measuring the amount of generated ATP, a known amount of ATP was injected into the base buffer after measurement. To measure the dependence of the ATP synthesis rate on the ADP or phosphate concentration, the phosphate and ADP concentrations were fixed at 10 and 1 mM, respectively. The pH of the mixture of acidified proteoliposome suspension and base buffer (pH_{out}) was directly measured using a glass electrode to determine ΔpH (= pH_{out} − pH_{in}). The ΔpH and ΔΨ dependences were measured by changing the pH and $[K^+]$ of the acidification and base buffers. ΔΨ was calculated by the Nernst equation using the difference in $[K^+]$ inside and outside the liposome, *i.e.* $2.3(k_BT/e)\log([K^+]_{out}/[K^+]_{in})$, where k_B is the Boltzmann constant, and e is the elementary charge. Measurements were carried out at 24–25 °C.

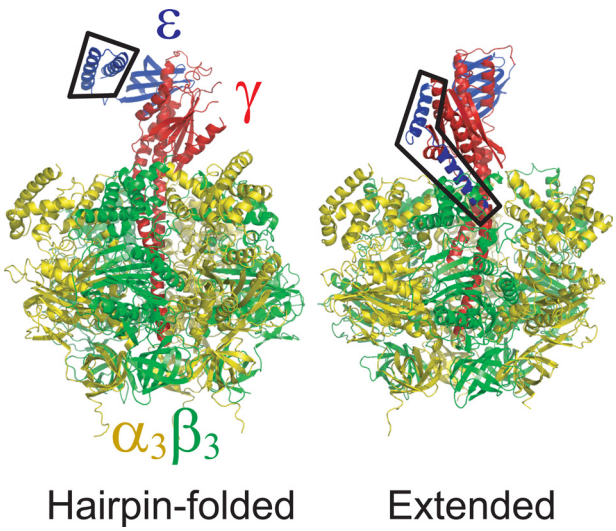

FIGURE 1. **Crystal structures of the ϵ subunit (*blue*) of EF_1 in the extended state (*right*, Protein Data Bank code 1JNV) (22) and the δ subunit (equivalent to bacterial ϵ) of F_1 from bovine mitochondria in the hairpin-folded state (*left*, Protein Data Bank code 1E79) (21).** The C-terminal α-helices of the ϵ subunit (enclosed by *black lines*) of EF_oF_1 were truncated by introducing a stop codon at the position of Asp-91.

Measurement of the ATP Hydrolysis Activity—The ATP hydrolysis activity of solubilized EF_oF_1 was measured with an ATP regeneration system using a UV-visible spectrophotometer (VP-550, Jasco). Various concentrations of ATP (Sigma) were added to the assay mixture (10 mM HEPES-NaOH (pH 7.5), 5 mM $MgSO_4$, 1 mM KCl, 0.3% (w/v) $C_{12}E_8$, 2.5 mM phosphoenolpyruvate, 0.1 mg/ml pyruvate kinase, 0.1 mg/ml lactate dehydrogenase, and 0.2 mM NADH) at 0 s, and this was followed by the addition of various concentrations of EF_oF_1 at 30 s. The NADH absorbance at 340 nm was monitored for 1200 s. The ATP hydrolysis rate was calculated from the time course of the change in [NADH] using a molecular extinction coefficient value of 6220 at 340 nm. Because the ATP hydrolysis activity gradually increased in the initial state after the addition of EF_oF_1, the maximum activity in the steady state at around 1000–1200 s was used for data analysis. Measurements were carried out at 24–25 °C.

RESULTS

ATP Synthesis by the $F_oF_1^{\epsilon\Delta C}$ Mutant of EF_oF_1 Reconstituted into the Liposome—The C-terminal α-helices of the ϵ subunit of EF_oF_1 were truncated by introducing a stop codon at Asp-91 (Fig. 1). The ATP synthesis activity of the truncated mutant ($F_oF_1^{\epsilon\Delta C}$) was compared in detail with that of the wild-type enzyme ($F_oF_1^{\epsilon WT}$). The expression level of $F_oF_1^{\epsilon\Delta C}$ was similar to that of $F_oF_1^{\epsilon WT}$ in the inverted membrane of RA1 strain *E. coli* (*unc*$^-$/*cyo*$^-$), and it was purified as a stable EF_oF_1 complex using the His tags introduced into the c subunits (Fig. 2*A*). No differences in concentration determination by the BCA assay and purity were observed between $F_oF_1^{\epsilon WT}$ and $F_oF_1^{\epsilon\Delta C}$. Purified EF_oF_1 was reconstituted into the liposome, and ATP synthesis activities driven by ΔpH and ΔΨ

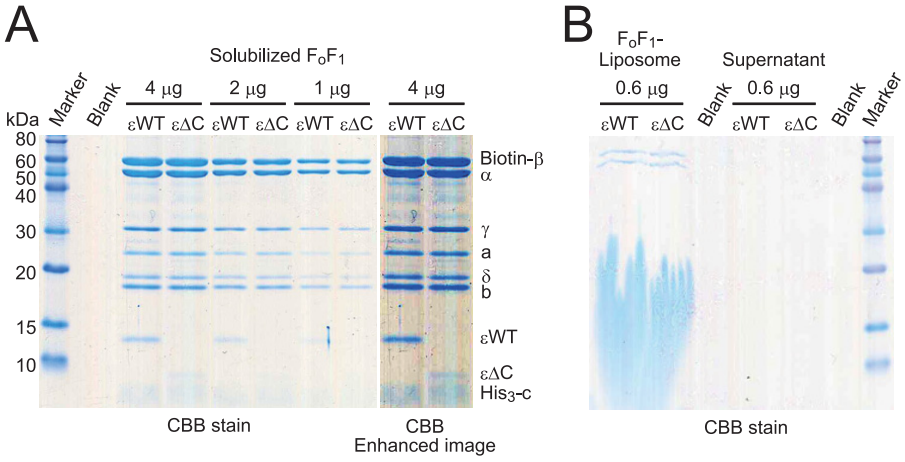

FIGURE 2. **EF_oF_1 purification and reconstitution into liposome.** *A*, SDS-PAGE of purified $F_oF_1^{\epsilon WT}$ and $F_oF_1^{\epsilon\Delta C}$. Concentrations were determined by the BCA assay, and different amounts of the proteins were applied and separated. No variations in concentration determination and purity were observed between $F_oF_1^{\epsilon WT}$ and $F_oF_1^{\epsilon\Delta C}$. *CBB*, Coomassie Brilliant Blue. *B*, SDS-PAGE of $F_oF_1^{\epsilon WT}$ and $F_oF_1^{\epsilon\Delta C}$ reconstituted into liposome. EF_oF_1-liposome suspension (0.6 μg of protein) and the supernatant after precipitation of EF_oF_1-liposome by ultracentrifugation were applied and separated. Virtually, all $F_oF_1^{\epsilon WT}$ and $F_oF_1^{\epsilon\Delta C}$ precipitated with liposome, indicating that reconstitution efficiencies of both enzymes were very high.

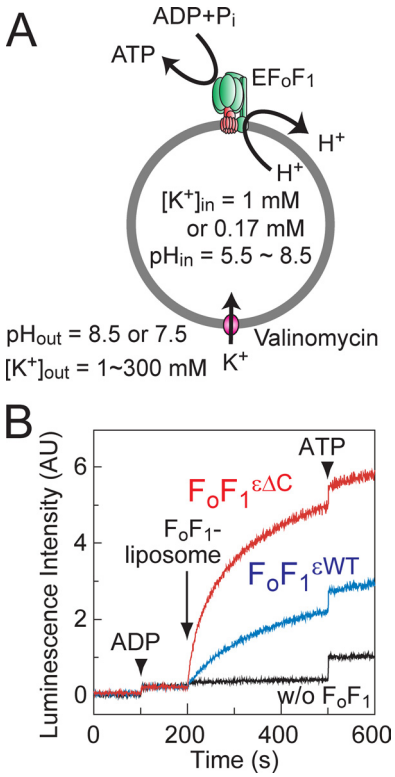

FIGURE 3. **Measurement of ATP synthesis by EF_oF_1 reconstituted into a liposome.** *A,* schematic illustration of the experimental system. *B,* examples of raw data at pH_{in} and pH_{out} values of 5.5 and 8.5, respectively ($\Delta pH = 3.0$), corresponding to 177 mV ($= 2.3(k_BT/e)\Delta pH$). $\Delta\Psi$ was generated by the difference in $[K^+]_{out}$ (30 mM) and $[K^+]_{in}$ (1 mM) in the presence of 36 nM valinomycin. $\Delta\Psi$ was calculated by the Nernst equation, *i.e.* $\Delta\Psi = 2.3(k_BT/e)\log([K^+]_{out}/[K^+]_{in})$, and corresponded to 87 mV. The proton motive force ($\Delta\mu$, 264 mV) was calculated by the equation $\Delta\mu = 2.3(k_BT/e)\Delta pH + \Delta\Psi$. The ATP synthesis rates of $F_oF_1^{\epsilon WT}$ (*blue*) and $F_oF_1^{\epsilon\Delta C}$ (*red*) and liposome without F_oF_1 (*black*), determined by linear fitting of the initial slope after addition of the F_oF_1 liposome, were 11, 49, and $<1\ s^{-1}$, respectively. The concentrations of ADP and P_i were 1 and 10 mM, respectively. Measurements were carried out at 24–25 °C. Final concentrations of EF_oF_1 were ~0.5 nM, and final concentrations of ATP added as standard were 200 nM.

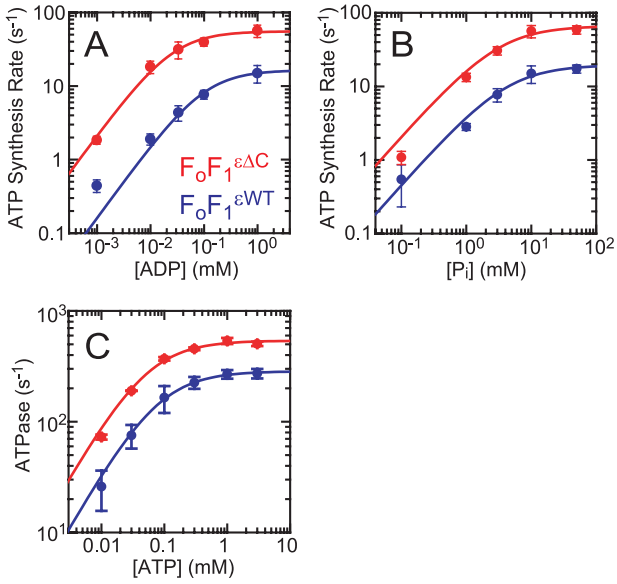

FIGURE 4. **ATP synthesis and hydrolysis rates of $F_oF_1^{\epsilon WT}$ (*blue*) and $F_oF_1^{\epsilon\Delta C}$ (*red*) as a function of the substrate concentration.** *A* and *B,* [ADP] (*A*) and $[P_i]$ (*B*) dependences of the ATP synthesis rate of EF_oF_1 liposome. $[P_i]$ (*A*), [ADP] (*B*), $\Delta\Psi$, and $2.3(k_BT/e)\Delta pH$ were set at 10 and 1 mM and 87 and 177 mV, respectively. *C,* [ATP] dependence of the ATP hydrolysis rate of solubilized EF_oF_1. Measurements were carried out four to six times (total of two independent preparations) for each data point at 24–25 °C.

were measured. Several methods have been proposed for reconstituting EF_oF_1 into liposomes, including the following: 1) reconstitution by detergent removal from a mixture of solubilized EF_oF_1 and liposome using Bio-Beads SM (36); 2) dialysis; and 3) reconstitution by diluting the detergent in solubilized EF_oF_1 with an excess amount of liposome and subsequent freeze-thaw. Because the last method resulted in the highest ATP synthesis activity (data not shown), we employed this method throughout this study. The reconstitution efficiencies were very high, and no differences were observed between $F_oF_1^{\epsilon WT}$ and $F_oF_1^{\epsilon\Delta C}$ (Fig. 2*B*). By using an excess of the liposome suspension, a high lipid/protein molar ratio was obtained ($\sim 2 \times 10^5$). The average protein/liposome ratio was less than unity, and most liposomes contained one or zero EF_oF_1 molecules. This was estimated by assuming that the liposome diameter is in the range 100–200 nm (Fig. 3*A*) (30, 35).

Examples of raw data obtained from the ATP synthesis experiments are shown in Fig. 3*B*. The amount of generated ATP was determined on the basis of the luminescence observed in the luciferin-luciferase reaction. The luminescence intensity was proportional to the ATP concentration in the reaction mixture under our experimental conditions (data not shown). Addition of ADP to the reaction mixture showed a slight increase in the luminescence intensity because of the ATP contamination in ADP, which was calculated to be ~0.05%. Under the "Discussion," we used the initial rate of ATP synthesis. As shown in Fig. 3*B*, $F_oF_1^{\epsilon\Delta C}$ exhibited a much higher rate (49 s^{-1}, *red line*) than $F_oF_1^{\epsilon WT}$ (11 s^{-1}, *blue line*), as reported earlier for TF_oF_1 in an inverted membrane (31). The observed differences were actually due to the removal of C-terminal α-helices of the ϵ subunit and not to variations in concentration determination, purity, and reconstitution efficiency between $F_oF_1^{\epsilon WT}$ and $F_oF_1^{\epsilon\Delta C}$ (Fig. 2). This result indicates that the C-terminal domain of ϵ suppresses the ATP synthesis activity. As a control, the time course of the liposome without EF_oF_1 is also shown ($<1\ s^{-1}$, Fig. 3*B*, *black line*), and the results indicate that the ATP was actually generated by EF_oF_1.

Dependence of ATP Synthesis and Hydrolysis Rates on the Substrate Concentration—The ATP synthesis rate was measured at various concentrations of ADP and P_i. The [substrate]-velocity plots for ADP and P_i showed that the ATP synthesis rates of $F_oF_1^{\epsilon WT}$ and $F_oF_1^{\epsilon\Delta C}$ obeyed Michaelis-Menten kinetics (Fig. 4, *A* and *B*). The values of the turnover number (k_{cat}) and Michaelis constant (K_m) are summarized in Table 1. The k_{cat} values of $F_oF_1^{\epsilon WT}$ for ADP and P_i were 0.29- and 0.30-fold the values of $F_oF_1^{\epsilon\Delta C}$, respectively (ratio shown in Table 1). Furthermore, in the case of $F_oF_1^{\epsilon WT}$, the Michaelis constants (K_m) were 4.0- (ADP) and 1.3-fold (P_i) higher than those of $F_oF_1^{\epsilon\Delta}$. These changes resulted in second-order rate constants (k_{cat}/K_m) of $F_oF_1^{\epsilon WT}$ that were 0.073- (ADP) and 0.23-fold (P_i) the values of $F_oF_1^{\epsilon\Delta}$.

The ATP hydrolysis rates of $F_oF_1^{\epsilon WT}$ and $F_oF_1^{\epsilon\Delta C}$ were also compared. The [substrate]-velocity plots of ATP hydrolysis also obeyed Michaelis-Menten kinetics (Fig. 4*C*). The k_{cat} and K_m values of $F_oF_1^{\epsilon WT}$ were 0.53- and 1.5-fold the values of $F_oF_1^{\epsilon\Delta C}$, respectively. Consequently, the k_{cat}/K_m ratio of $F_oF_1^{\epsilon WT}$ was 0.38-fold that of $F_oF_1^{\epsilon\Delta C}$ (Table 2).

TABLE 1

Kinetic parameters for ATP synthesis of $F_oF_1^{\epsilon WT}$ and $F_oF_1^{\epsilon\Delta C}$ reconstituted into liposomes

Measurements were carried out at 24–25 °C. Data were measured using EF_oF_1 liposome. pH_{in} and pH_{out} were 5.5 and 8.5, respectively (ΔpH 3.0), corresponding to 177 mV (= 2.3(k_BT/e) ΔpH). $[K^+]_{in}$ and $[K^+]_{out}$ were 1 and 30 mM, respectively, corresponding to ΔΨ of 87 mV (= 2.3(k_BT/e)log($[K^+]_{out}/[K^+]_{in}$)). The F_1 unit of all F_oF_1 motors was assumed to be oriented toward the exterior of the liposomal membrane.

Substrates varied	ADP[a]			P_i[b]		
	k_{cat}	$K_{m(ADP)}$	$k_{cat}/K_{m(ADP)}$	k_{cat}	$K_{m(P_i)}$	$k_{cat}/K_{m(P_i)}$
	s^{-1}	M	$M^{-1}s^{-1}$	s^{-1}	M	$M^{-1}s^{-1}$
$F_oF_1^{\epsilon WT}$	16 ± 0.6	(1.0 ± 0.12) × 10^{-4}	1.6 × 10^5	20 ± 1.2	(4.2 ± 0.92) × 10^{-3}	4.8 × 10^3
$F_oF_1^{\epsilon\Delta C}$	55 ± 3.2	(2.5 ± 0.58) × 10^{-5}	2.2 × 10^6	66 ± 5.0	(3.2 ± 0.86) × 10^{-3}	2.1 × 10^4
Ratio[c]	0.29	4.0	0.073	0.30	1.3	0.23

[a] $[P_i]$ was 10 mM.
[b] [ADP] was 1 mM.
[c] The values for $F_oF_1^{\epsilon WT}$ were divided by those for $F_oF_1^{\epsilon\Delta C}$.

TABLE 2

Kinetic parameters for ATP hydrolysis of solubilized $F_oF_1^{\epsilon WT}$ and $F_oF_1^{\epsilon\Delta C}$

Measurements were carried out at 24–25 °C.

	k_{cat}	$K_{m(ATP)}$	$k_{cat}/K_{m(ATP)}$
	s^{-1}	M	$M^{-1}s^{-1}$
$F_oF_1^{\epsilon WT}$	285 ± 4.4	(7.8 ± 0.54) × 10^{-5}	3.8 × 10^6
$F_oF_1^{\epsilon\Delta C}$	539 ± 15.0	(5.2 ± 0.68) × 10^{-5}	1.0 × 10^7
Ratio[a]	0.53	1.5	0.38

[a] The values for $F_oF_1^{\epsilon WT}$ were divided by those for $F_oF_1^{\epsilon\Delta C}$.

Dependence of the ATP Synthesis Rate on ΔpH and ΔΨ—In the chemiosmotic theory first proposed by Mitchell (37), Δμ consists of ΔpH and ΔΨ, *i.e.* Δμ = 2.3(k_BT/e)ΔpH + ΔΨ. Several studies on F_oF_1 from *E. coli*, *Propionigenium modestum*, and the chloroplast have reported that the dependence of the ATP synthesis rate on the amplitude of ΔpH and ΔΨ is kinetically different (38–40). Previous results have suggested the possibility that elementary steps of the ATP synthesis reaction are affected in different ways by ΔpH and ΔΨ, although the mechanism is still unclear. Therefore, we measured the ATP synthesis rates using various combinations of ΔpH and ΔΨ. Fig. 5*A* shows contour plots of the ATP synthesis rate as a function of ΔpH and ΔΨ. Although the absolute values of the rates of $F_oF_1^{\epsilon WT}$ and $F_oF_1^{\epsilon\Delta C}$ differed, their dependences on ΔpH and ΔΨ were similar. Applying ΔpH resulted in a higher ATP synthesis rate than when the same amplitude of ΔΨ was applied in both $F_oF_1^{\epsilon WT}$ and $F_oF_1^{\epsilon\Delta C}$. This result was apparently inconsistent with previous studies reporting that ΔΨ was more effective than ΔpH in driving ATP synthesis by EF_oF_1 (38–40). So far, we have no clear idea why ΔpH was more effective in our experiment. Because we did not use the dicarboxylic acid such as maleic acid and succinic acid as the acidification buffer, concomitant formation of ΔΨ was not plausible (38, 40). Other factors such as different compositions of the liposome and the reaction solution might affect the dependence of ΔpH and ΔΨ.

Under our experimental conditions, [ADP] and $[P_i]$ were 1 and 10 mM, respectively, and ATP contamination in ADP was ~0.05%. By using the standard Gibbs free energy value of 14.9 k_BT (37 kJ/mol) (41), this corresponds to Gibbs free energy for ATP hydrolysis of −11.9 k_BT (= −14.9 k_BT + k_BT ln($10^{-3} \times 10^{-2}/5 \times 10^{-7}$)) or −306 mV. Thus, if we assume that 3 ATP molecules are synthesized and 10 protons are transported per turn (42), the potential difference that counteracts single proton translocation, or the value of Δμ at the ATP synthesis/hydrolysis equilibrium point, will be 92 mV (= (306 mV × 3)/10). We next plotted the dependence of the ATP synthesis rate on ΔΨ and ΔpH when 2.3 k_BT/e ΔpH and ΔΨ were fixed around this equilibrium value (89 and 87 mV, respectively) (Fig. 5*B*, corresponds to the *dashed lines* in Fig. 5*A*). As expected, no ATP synthesis was observed around the equilibrium value. When ΔpH increased, the ATP synthesis rate increased nonlinearly in the pH_{in} range from 5.5 to 8.5 (Fig. 5*B*, *circles*). The Δμ has a dimension equivalent to energy. Therefore, the nonlinear increase can be explained if we assume that the ATP synthesis rate changes according to the equation that resembles the Arrhenius equation in which the rate increases exponentially as the activation energy decreases.

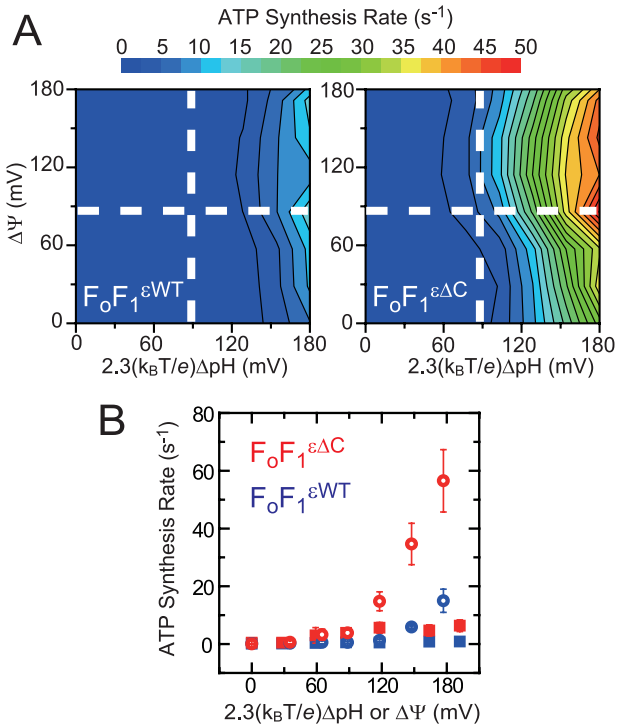

FIGURE 5. **Dependence of the ATP synthesis rates on various combinations of ΔpH and ΔΨ.** *A*, contour plots of the ATP synthesis rates of $F_oF_1^{\epsilon WT}$ (*left*) and $F_oF_1^{\epsilon\Delta C}$ (*right*) as functions of ΔpH and ΔΨ. ATP synthesis rates are indicated by different colors shown at the *top*. *B*, dependence of the ATP synthesis rate of $F_oF_1^{\epsilon WT}$ (*blue*) and $F_oF_1^{\epsilon\Delta C}$ (*red*) on ΔpH (*circles*) and ΔΨ (*squares*) when ΔΨ and 2.3(k_BT/e)ΔpH were fixed at 89 and 87 mV, respectively. [ADP] and $[P_i]$ were set at 1 and 10 mM, respectively. Measurements were carried out two to six times (total of two independent preparations) for each data point at 24–25 °C.

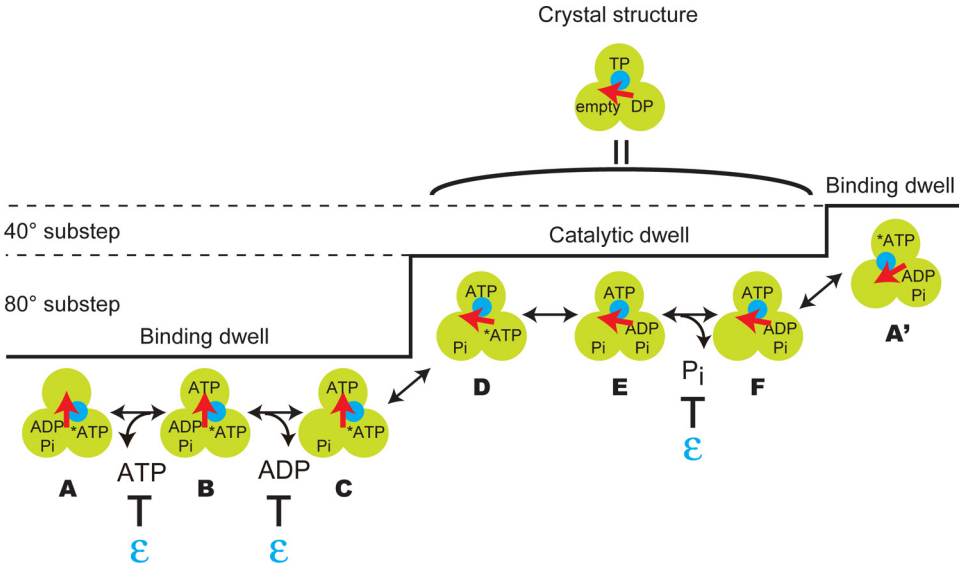

FIGURE 6. **Summary of the results of this study together with our recently proposed model of mechanochemical coupling.** The *green circles, red arrow*, and *blue circle* represent the β, γ, and ϵ subunits, respectively. In this model, γ rotates 120° by single ATP hydrolysis (44), and each 120° step is further divided into 80° and 40° substeps (45). The 80° substep is triggered upon ATP binding, whereas the 40° substep occurs after covalent bond cleavage (45, 46). Dwells before the 80° and 40° substeps are termed the binding dwell and catalytic dwell, respectively. ADP release and P_i release occur before (or during) the 80° and 40° substeps, respectively (47, 48). States in catalytic dwell (*D–F*) correspond to the crystal structures of F_1 (51). **ATP* represents ATP that is tightly bound to the β subunit but is not hydrolyzed. Although the C-terminal domain of ϵ in the extended state interacts with only β_{TP} in the crystal structure (Fig. 1) (22), our results strongly suggest that this domain suppresses multiple elementary steps of ATP synthesis/hydrolysis that are executed in multiple β subunits. A model that explains our results is proposed under the "Discussion."

DISCUSSION

Correlation between the Conformation of the ϵ Subunit of EF_oF_1 and Catalytic Activity—Truncation of the C-terminal domain of the ϵ subunit of EF_oF_1 ($F_oF_1^{\epsilon\Delta C}$) resulted in increased ATP synthesis and hydrolysis activities (Fig. 4 and Tables 1 and 2). The enhancement was observed under all conditions studied. This indicates that the C-terminal domain of the ϵ subunit of EF_oF_1 suppresses both ATP synthesis and hydrolysis. As described above, ϵ can adopt either of two different conformations, hairpin-folded or extended (Fig. 1). The crystal structure of F_1 with the hairpin-folded ϵ shows that ϵ does not have any direct interaction with the catalytic $\alpha_3\beta_3$ ring, whereas in the EF_1 crystal structure with the extended ϵ, the C-terminal helix of ϵ interacts with the $\alpha_3\beta_3$ ring. Therefore, the extended form is thought to be responsible for the inhibitory effect of ϵ. Previous experiments involving the cross-linking of EF_oF_1 and TF_oF_1 showed that the ATP hydrolysis activity was inhibited when ϵ was fixed in the extended state (26, 27). These results are consistent with the present results. On the other hand in the previous studies, there was no significant change in the ATP synthesis activity when ϵ was fixed in the extended state. This observation can be explained by assuming that ϵ mostly adopts the extended form under conditions of ATP synthesis, as suggested earlier (27). Thus, although the apparent inhibitory effect of ϵ differs during ATP hydrolysis and synthesis, probably as a result of the different ratios of the extended *versus* hairpin-folded forms, the extended form of ϵ is the primary inhibitory state under both ATP synthesis and hydrolysis conditions, and the C-terminal domain is responsible for inhibition.

Mechanism of Inhibition of ATP Synthesis by the C-terminal Domain of the ϵ Subunit of EF_oF_1 in the Extended State—During both ATP synthesis and hydrolysis, $F_oF_1^{\epsilon WT}$ exhibited lower k_{cat} and k_{cat}/K_m and higher K_m values than those of $F_oF_1^{\epsilon\Delta C}$ (Fig. 4 and Tables 1 and 2). Higher K_m and lower k_{cat}/K_m values of $F_oF_1^{\epsilon WT}$ in comparison with those of $F_oF_1^{\epsilon\Delta C}$ indicate decreased substrate affinity and rate of substrate binding, respectively. Furthermore, the lower k_{cat} value of $F_oF_1^{\epsilon WT}$ in comparison with that of $F_oF_1^{\epsilon\Delta C}$ indicates a decreased rate of covalent bond formation/cleavage or product release.

With respect to ATP hydrolysis, our result is consistent with that of a previous study in which the decreased affinity of MgATP in the presence of the ϵ subunit was demonstrated (11). A previous study also reported that the ϵ subunit of EF_1 had no effect on the equilibrium between ATP and ADP·P_i but reduced the rate of product release under unisite ATP hydrolysis conditions (12). If this is also the case in multisite catalysis, ϵ will not affect covalent bond formation/cleavage, and product release will be slowed. In the case of ATP synthesis, a previous study proposed that the energy of $\Delta\mu$ is mainly used for product release (43), suggesting that the product release step is rate-limiting. This is consistent with the assumption that it is the product release step that is slowed in $F_oF_1^{\epsilon WT}$ and not the covalent bond formation/cleavage step. In our study, the dependence of the ATP synthesis rate on various combinations of ΔpH and ΔΨ was similar in both $F_oF_1^{\epsilon WT}$ and $F_oF_1^{\epsilon\Delta C}$ (Fig. 5*A*). This suggests that the C-terminal domain of ϵ in the extended state does not change the rate-limiting step of ATP synthesis. Furthermore, it is consistent with the notion that multiple elementary steps of the ATP synthesis reaction are slowed. Thus, during both ATP synthesis and hydrolysis, the rates of substrate binding and product release appear to be suppressed by the C-terminal domain of ϵ.

However, when the reversibility of the reaction is considered, there is a problem in explaining our results. To examine this, we discuss our results based on our recently proposed model of mechanochemical coupling of F_1 (Fig. 6) (44–48). During ATP hydrolysis, the lower k_{cat} of value $F_oF_1^{\epsilon WT}$ in comparison with that of $F_oF_1^{\epsilon\Delta C}$ corresponds to a lower rate of product (ADP or P_i) release (Fig. 6, $B \rightarrow C$ or $E \rightarrow F$). Slow ADP or P_i release generally results in high affinity, but this is inconsistent with the higher K_m value of $F_oF_1^{\epsilon WT}$ for ADP or P_i in comparison with the corresponding values of $F_oF_1^{\epsilon\Delta C}$ during ATP synthesis. Similarly, although a lower k_{cat} value of $F_oF_1^{\epsilon WT}$ in comparison with that of $F_oF_1^{\epsilon\Delta C}$ during ATP synthesis corresponds to a

lower ATP release rate (Fig. 6, $B \rightarrow A$), this result also appears to be inconsistent with the higher K_m value of $F_oF_1^{\epsilon WT}$ for ATP in comparison with that of $F_oF_1^{\epsilon\Delta C}$ during ATP hydrolysis.

From a structural point of view, there is another problem in explaining our results. As shown in Fig. 6, each β subunit sequentially executes elementary steps of the reaction and is always in a different chemical state from the other subunits (49, 50). In the low resolution crystal structure of EF_1 (Fig. 1), the C-terminal domain of ε in the extended state interacts with only one β subunit bound to the ATP analog (Fig. 6, β_{TP} in crystal structure), although there must be some displacement due to steric hindrance in the structural model (22). We recently proved that the crystal structures of F_1 correspond to states *D–F* in Fig. 6 (states in catalytic dwell), and β_{TP} corresponds to the β subunit immediately after ATP binding (51). Thus, ε would affect only ATP binding and release by direct interaction with β_{TP}. Even if we consider states A to C in Fig. 5 (states in binding dwell), it seems difficult for ε to simultaneously interact with multiple β subunits and to directly suppress other elementary steps of the reaction such as ADP and P_i binding/release that occur in other β subunits.

These apparent difficulties can be explained on the basis of the following model in which we assume that the rates of elementary steps of the reaction executed in each β subunit are modulated not by direct interaction with ε but by the rotary angle of γ (rotor). The C-terminal domain of ε in the extended state increases the diameter of the rotor (γ and ε) inserted into the $\alpha_3\beta_3$ ring and restricts its rotation. This results in lower rates of multiple elementary steps during both ATP synthesis and hydrolysis in multiple β subunits. Our assumption that the rate of the elementary step is dependent on the rotary angle of γ is supported by our previous single-molecule experiments in which we reported that the rate of ADP release from the MgADP-inhibited $\alpha_3\beta_3\gamma$ subcomplex of TF_1 strongly depended on the rotary angle of γ (52). This suggests that the rate of ADP release (Fig. 6, $B \rightarrow C$) in active F_1 is also dependent on the angle of γ. Furthermore, the rates of ATP binding/release (Fig. 6, $A \leftrightarrow B$) are strongly dependent on the rotary angle of γ in an actively rotating TF_1 $\alpha_3\beta_3\gamma$ subcomplex.[5] Interestingly, our unpublished results[5] also indicate that the rates of covalent bond formation/cleavage (Fig. 6, $D \leftrightarrow E$) are less dependent on the angle of γ. Taking this into consideration, the results of a previous study in which it was reported that this step was unaffected by ε (12) are consistent with our assumption that ε restricts the rotation of γ.

Our model predicts that the dwell times before the 80° and 40° substeps will become longer when the rotation of EF_1 is assayed in the presence of ε. Previous single molecule observations of EF_1 rotation driven by ATP hydrolysis have shown that ε increases the frequency and duration of the transient pause and results in decreased rotation speed (53). However, in the previous study, the pause angles were not resolved. Detailed analysis of pause angles and dwell times will provide further insights into the mechanism of inhibition by the ε subunit.

[5] R. Watanabe, D. Okuno, S. Sakakihara, K. Shimabukuro, R. Iino, M. Yoshida, and H. Noji, unpublished results.

Effect of the C-terminal Domain of ε on the Efficiency of the Mechanochemical Coupling during ATP Synthesis—In this study, $F_oF_1^{\epsilon\Delta C}$ showed a higher rate of ATP synthesis than $F_oF_1^{\epsilon WT}$. However, we could not directly assess the coupling efficiency between the mechanical rotation of γ and each elementary step of the reaction. A high ATP synthesis rate does not necessarily indicate high coupling efficiency. As proposed previously (54), we can expect a situation in which the rotation rate is faster but the coupling efficiency of $F_oF_1^{\epsilon\Delta C}$ is lower than that of $F_oF_1^{\epsilon WT}$ during ATP synthesis. We previously reported that reconstitution of ε into the $\alpha_3\beta_3\gamma$ subcomplex of TF_1 improved the coupling efficiency of ATP synthesis when γ was forcibly rotated with magnetic tweezers (55, 56). The role of the C-terminal domain of ε in the coupling efficiency of ATP synthesis can be directly investigated by single molecule manipulation of $F_oF_1^{\epsilon\Delta C}$ or the $\alpha_3\beta_3\gamma$ subcomplex of F_1 reconstituted with C-terminal truncated ε.

Acknowledgments—We thank Drs. Nobuhito Sone, Masatoshi Toei, Masahiro Nakano, and Ken Yokoyama for technical advice and members of the Noji laboratory for helpful discussions.

REFERENCES

1. Boyer, P. D. (1997) *Annu. Rev. Biochem.* **66,** 717–749
2. Senior, A. E., Nadanaciva, S., and Weber, J. (2002) *Biochim. Biophys. Acta* **1553,** 188–211
3. Capaldi, R. A., and Aggeler, R. (2002) *Trends Biochem. Sci.* **27,** 154–160
4. Noji, H., Yasuda, R., Yoshida, M., and Kinosita, K., Jr. (1997) *Nature* **386,** 299–302
5. Yoshida, M., Muneyuki, E., and Hisabori, T. (2001) *Nat. Rev. Mol. Cell Biol.* **2,** 669–677
6. Kinosita, K., Jr., Adachi, K., and Itoh, H. (2004) *Annu. Rev. Biophys. Biomol. Struct.* **33,** 245–268
7. Sternweis, P. C., and Smith, J. B. (1980) *Biochemistry* **19,** 526–531
8. Capaldi, R. A., and Schulenberg, B. (2000) *Biochim. Biophys. Acta* **1458,** 263–269
9. Vik, S. B. (2000) *J. Bioenerg. Biomembr.* **32,** 485–491
10. Feniouk, B. A., Suzuki, T., and Yoshida, M. (2006) *Biochim. Biophys. Acta* **1757,** 326–338
11. Weber, J., Dunn, S. D., and Senior, A. E. (1999) *J. Biol. Chem.* **274,** 19124–19128
12. Dunn, S. D., Zadorozny, V. D., Tozer, R. G., and Orr, L. E. (1987) *Biochemistry* **26,** 4488–4493
13. Mendel-Hartvig, J., and Capaldi, R. A. (1991) *Biochemistry* **30,** 10987–10991
14. Kato, Y., Matsui, T., Tanaka, N., Muneyuki, E., Hisabori, T., and Yoshida, M. (1997) *J. Biol. Chem.* **272,** 24906–24912
15. Kato-Yamada, Y., Bald, D., Koike, M., Motohashi, K., Hisabori, T., and Yoshida, M. (1999) *J. Biol. Chem.* **274,** 33991–33994
16. Xiong, H., Zhang, D., and Vik, S. B. (1998) *Biochemistry* **37,** 16423–16429
17. Wilkens, S., Dahlquist, F. W., McIntosh, L. P., Donaldson, L. W., and Capaldi, R. A. (1995) *Nat. Struct. Biol.* **2,** 961–967
18. Uhlin, U., Cox, G. B., and Guss, J. M. (1997) *Structure* **5,** 1219–1230
19. Wilkens, S., and Capaldi, R. A. (1998) *J. Biol. Chem.* **273,** 26645–26651
20. Rodgers, A. J., and Wilce, M. C. (2000) *Nat. Struct. Biol.* **7,** 1051–1054
21. Gibbons, C., Montgomery, M. G., Leslie, A. G., and Walker, J. E. (2000) *Nat. Struct. Biol.* **7,** 1055–1061
22. Hausrath, A. C., Capaldi, R. A., and Matthews, B. W. (2001) *J. Biol. Chem.* **276,** 47227–47232
23. Ganti, S., and Vik, S. B. (2007) *J. Bioenerg. Biomembr.* **39,** 99–107
24. Schulenberg, B., and Capaldi, R. A. (1999) *J. Biol. Chem.* **274,** 28351–28355
25. Kato-Yamada, Y., Yoshida, M., and Hisabori, T. (2000) *J. Biol. Chem.* **275,**

35746–35750
26. Tsunoda, S. P., Rodgers, A. J., Aggeler, R., Wilce, M. C., Yoshida, M., and Capaldi, R. A. (2001) *Proc. Natl. Acad. Sci. U.S.A.* **98,** 6560–6564
27. Suzuki, T., Murakami, T., Iino, R., Suzuki, J., Ono, S., Shirakihara, Y., and Yoshida, M. (2003) *J. Biol. Chem.* **278,** 46840–46846
28. Bulygin, V. V., Duncan, T. M., and Cross, R. L. (2004) *J. Biol. Chem.* **279,** 35616–35621
29. Iino, R., Murakami, T., Iizuka, S., Kato-Yamada, Y., Suzuki, T., and Yoshida, M. (2005) *J. Biol. Chem.* **280,** 40130–40134
30. Zimmermann, B., Diez, M., Zarrabi, N., Gräber, P., and Börsch, M. (2005) *EMBO J.* **24,** 2053–2063
31. Masaike, T., Suzuki, T., Tsunoda, S. P., Konno, H., and Yoshida, M. (2006) *Biochem. Biophys. Res. Commun.* **342,** 800–807
32. Aggeler, R., Chicas-Cruz, K., Cai, S. X., Keana, J. F., and Capaldi, R. A. (1992) *Biochemistry* **31,** 2956–2961
33. Cronan, J. E., Jr. (1990) *J. Biol. Chem.* **265,** 10327–10333
34. Aggeler, R., Ogilvie, I., and Capaldi, R. A. (1997) *J. Biol. Chem.* **272,** 19621–19624
35. Toei, M., Gerle, C., Nakano, M., Tani, K., Gyobu, N., Tamakoshi, M., Sone, N., Yoshida, M., Fujiyoshi, Y., Mitsuoka, K., and Yokoyama, K. (2007) *Proc. Natl. Acad. Sci. U.S.A.* **104,** 20256–20261
36. Fischer, S., Etzold, C., Turina, P., Deckers-Hebestreit, G., Altendorf, K., and Gräber, P. (1994) *Eur. J. Biochem.* **225,** 167–172
37. Mitchell, P. (1961) *Nature* **191,** 144–148
38. Kaim, G., and Dimroth, P. (1998) *FEBS Lett.* **434,** 57–60
39. Fischer, S., and Gräber, P. (1999) *FEBS Lett.* **457,** 327–332
40. Kaim, G., and Dimroth, P. (1999) *EMBO J.* **18,** 4118–4127
41. Turina, P., Samoray, D., and Gräber, P. (2003) *EMBO J.* **22,** 418–426
42. Jiang, W., Hermolin, J., and Fillingame, R. H. (2001) *Proc. Natl. Acad. Sci. U.S.A.* **98,** 4966–4971
43. Boyer, P. D., Cross, R. L., and Momsen, W. (1973) *Proc. Natl. Acad. Sci. U.S.A.* **70,** 2837–2839
44. Yasuda, R., Noji, H., Kinosita, K., Jr., and Yoshida, M. (1998) *Cell* **93,** 1117–1124
45. Yasuda, R., Noji, H., Yoshida, M., Kinosita, K., Jr., and Itoh, H. (2001) *Nature* **410,** 898–904
46. Shimabukuro, K., Yasuda, R., Muneyuki, E., Hara, K. Y., Kinosita, K., Jr., and Yoshida, M. (2003) *Proc. Natl. Acad. Sci. U.S.A.* **100,** 14731–14736
47. Adachi, K., Oiwa, K., Nishizaka, T., Furuike, S., Noji, H., Itoh, H., Yoshida, M., and Kinosita, K., Jr. (2007) *Cell* **130,** 309–321
48. Watanabe, R., Iino, R., Shimabukuro, K., Yoshida, M., and Noji, H. (2008) *EMBO Rep.* **9,** 84–90
49. Ariga, T., Muneyuki, E., and Yoshida, M. (2007) *Nat. Struct. Mol. Biol.* **14,** 841–846
50. Masaike, T., Koyama-Horibe, F., Oiwa, K., Yoshida, M., and Nishizaka, T. (2008) *Nat. Struct. Mol. Biol.* **15,** 1326–1333
51. Okuno, D., Fujisawa, R., Iino, R., Hirono-Hara, Y., Imamura, H., and Noji, H. (2008) *Proc. Natl. Acad. Sci. U.S.A.* **105,** 20722–20727
52. Hirono-Hara, Y., Ishizuka, K., Kinosita, K., Jr., Yoshida, M., and Noji, H. (2005) *Proc. Natl. Acad. Sci. U.S.A.* **102,** 4288–4293
53. Nakanishi-Matsui, M., Kashiwagi, S., Hosokawa, H., Cipriano, D. J., Dunn, S. D., Wada, Y., and Futai, M. (2006) *J. Biol. Chem.* **281,** 4126–4131
54. Cipriano, D. J., and Dunn, S. D. (2006) *J. Biol. Chem.* **281,** 501–507
55. Rondelez, Y., Tresset, G., Nakashima, T., Kato-Yamada, Y., Fujita, H., Takeuchi, S., and Noji, H. (2005) *Nature* **433,** 773–777
56. Iino, R., Rondelez, Y., Yoshida, M., and Noji, H. (2005) *J. Bioenerg. Biomembr.* **37,** 451–454